

Neutrinoless double- β decay of deformed nuclei within quasiparticle random-phase approximation with a realistic interaction

Dong-Liang Fang, Amand Faessler, and Vadim Rodin*

Institut für Theoretische Physik, Universität Tübingen, D-72076 Tübingen, Germany

Fedor Šimkovic

BLTP, JINR, Dubna, Russia and Department of Nuclear Physics, Comenius University, SK-842 15 Bratislava, Slovakia

(Received 12 January 2011; published 25 March 2011)

In this paper a microscopic approach to calculation of the nuclear matrix element $M^{0\nu}$ for neutrinoless double- β decay with an account for nuclear deformation is presented in length and applied for ^{76}Ge , ^{150}Nd , and ^{160}Gd . The proton-neutron quasiparticle random-phase approximation with a realistic residual interaction (the Brueckner G matrix derived from the charge-depending Bonn nucleon-nucleon potential) is used as the underlying nuclear structure model. The effects of the short-range correlations and the quenching of the axial vector coupling constant g_A are analyzed. The results suggest that neutrinoless double- β decay of ^{150}Nd , to be measured soon by the SNO+ Collaboration, may provide one of the best probes of the Majorana neutrino mass. This confirms our preliminary conclusion in Fang *et al.* [Phys. Rev. C **82**, 051301(R) (2010)].

DOI: 10.1103/PhysRevC.83.034320

PACS number(s): 23.40.Bw, 21.60.-n, 23.40.Hc, 27.70.+q

I. INTRODUCTION

Neutrinoless double- β decay ($0\nu\beta\beta$ decay) is a second-order nuclear weak decay process with the emission of two electrons only [1–3]: $(A, Z) \rightarrow (A, Z + 2) + 2e^-$. This process is forbidden in the standard model (SM) of electroweak interaction since it violates the conservation of the total lepton number. The observation of $0\nu\beta\beta$ decay will immediately prove the neutrino to be identical to its antiparticle (a Majorana particle) as ensured by the Schechter-Valle theorem [4]. Thereby, $0\nu\beta\beta$ decay offers the only feasible way to test the charge-conjugation property of the neutrinos. In addition, the existence of $0\nu\beta\beta$ decay requires that the neutrino is a massive particle.

The fact that the neutrinos have nonvanishing masses has firmly been established by neutrino oscillation experiments (see, e.g., Ref. [5]). However, the oscillation experiments cannot in principle measure the absolute scale of the neutrino masses. One of the possible ways to probe the absolute neutrino masses at the level of tens of meV is to study $0\nu\beta\beta$ decay. Provided the corresponding $0\nu\beta\beta$ -decay rates are accurately measured, a reliable nuclear matrix element (NME) $M^{0\nu}$ will be needed to deduce the effective Majorana neutrino mass from the experimental half-lives of the decay.

One of the best candidates for searching $0\nu\beta\beta$ decay is ^{150}Nd since it has the second highest endpoint, $Q_{\beta\beta} = 3.37$ MeV, and the largest phase-space factor for the decay (about 33 times larger than that for ^{76}Ge , see, e.g., [1]). The SNO+ experiment at the Sudbury Neutrino Observatory will use a Nd-loaded scintillator to search for neutrinoless double- β decay by looking for a distortion in the energy spectrum of decays at the endpoint [6]. SNO+ will be filled with 780 tons of liquid scintillator. The planned loading of 0.1% of the natural Nd translates into 43.6 kg of the isotope

^{150}Nd . It is expected to achieve the sensitivity of $T_{1/2}^{0\nu} \simeq 5 \times 10^{24}$ yr after one year of running, with the best final value of about 3–4 times longer (without enrichment of the dissolved Nd). With the NME $M^{0\nu} = 4.74$ of Ref. [7], obtained within the proton-neutron quasiparticle random-phase approximation (QRPA) with neglect of deformation, already the initial phase of SNO+ will be able to probe $m_{\beta\beta} \approx 100$ meV, and will finally be able to achieve sensitivity of $m_{\beta\beta} \approx 50$ meV corresponding to the inverse hierarchy (IH) of the neutrino mass spectrum.

However, ^{150}Nd is well known to be a rather strongly deformed nucleus. This strongly hinders a reliable theoretical evaluation of the corresponding $0\nu\beta\beta$ -decay NME; for instance, it does not seem feasible in the near future to reliably treat this nucleus within the large-scale nuclear shell model (LSSM), see, e.g., Ref. [8]. Recently, more phenomenological approaches like the pseudo-SU(3) model [9], the projected Hartree-Fock-Bogoliubov (PHFB) approach [10], the interacting boson model (IBM-2) [11], and the generator coordinate method with particle number and angular momentum projection (GCM+PNAMP) [12] have been employed to calculate $M^{0\nu}$ for strongly deformed heavy nuclei (a comparative analysis of different approximations involved in some of the models can be found in Ref. [13]). The results of these models generally reveal a substantial suppression of $M^{0\nu}$ for ^{150}Nd as compared with the QRPA result of Ref. [7] where ^{150}Nd and ^{150}Sm were treated as spherical nuclei. However, the calculated NME $M^{0\nu}$ for ^{150}Nd reveal rather significant spread.

One of the most up-to-date microscopic ways to describe the effect of nuclear deformation on $\beta\beta$ -decay NME $M^{2\nu}$ and $M^{0\nu}$ is provided by the QRPA. In Refs. [14–16] a QRPA approach for calculating $M^{2\nu}$ in deformed nuclei has been developed. Theoretical interpretation of the experimental NME $M_{\text{exp}}^{2\nu}$ which have been obtained for a dozen of nuclei [17] provides a test of different theoretical methods. It was demonstrated in Refs. [14–16] that deformation introduces a

*vadim.rodin@uni-tuebingen.de

mechanism of suppression of the $M^{2\nu}$ matrix element which gets stronger when deformations of the initial and final nuclei differ from each other. A similar dependence of the suppression of both $M^{2\nu}$ and $M^{0\nu}$ matrix elements on the difference in deformations has been found in the PHFB [10] and the LSSM [8].

In the previous Rapid Communication [18], we reported on the first QRPA calculation of $M^{0\nu}$ for ^{150}Nd with an account for nuclear deformation. The calculation showed a suppression of $M^{0\nu}$ by about 40% as compared with our previous QRPA result for ^{150}Nd [7] that was obtained with neglect of deformation. In this paper we give the details of the calculation of Ref. [18], and also include different nuclei in the analysis. In addition, the effects of the short-range correlations and the quenching of the axial vector coupling constant g_A are considered. Making use of the newest NME, one may conclude that $0\nu\beta\beta$ decay of ^{150}Nd , to be searched for by the SNO+ Collaboration soon, provides one of the best sensitivities to the Majorana neutrino mass and may approach the IH region of the neutrino mass spectrum.

II. FORMALISM

For the light Majorana neutrino exchange mechanism, the inverse $0\nu\beta\beta$ -decay lifetime is given by the product of three factors:

$$(T_{1/2}^{0\nu})^{-1} = G^{0\nu} |M'^{0\nu}|^2 m_{\beta\beta}^2, \quad (1)$$

where $G^{0\nu}$ is a calculable phase-space factor, $M'^{0\nu}$ is the $0\nu\beta\beta$ nuclear matrix element, and $m_{\beta\beta}$ is the (nucleus-independent) “effective Majorana neutrino mass” which, in standard notation [19], reads

$$m_{\beta\beta} = \left| \sum_{i=1}^3 m_i U_{ei}^2 \right|, \quad (2)$$

m_i and U_{ei} being the neutrino masses and the ν_e mixing matrix elements, respectively. The NME includes both Fermi (F) and Gamow-Teller (GT) transitions, plus a small tensor (T) contribution [2],

$$M'^{0\nu} = \left(\frac{g_A}{1.25} \right)^2 \left(-M_F^{0\nu} \frac{g_V^2}{g_A^2} + M_{GT}^{0\nu} + M_T^{0\nu} \right). \quad (3)$$

In the above expression, g_A is the effective axial coupling in nuclear matter, not necessarily equal to its “bare” free-nucleon value $g_A \simeq 1.25$. We note that for $g_A = 1.25$ nuclear matrix element $M'^{0\nu}$ coincides with the standard definition $M^{0\nu} = -M_F^{0\nu} \frac{g_V^2}{g_A^2} + M_{GT}^{0\nu} + M_T^{0\nu}$. With the conventional prefactor $\propto g_A^2$ in Eq. (3), the phase space $G^{0\nu}$ becomes independent of g_A .

The NME $M^{0\nu}$ for strongly deformed, axially symmetric nuclei can be most conveniently calculated within the QRPA in the intrinsic coordinate system associated with the rotating nucleus. This employs the adiabatic Bohr-Mottelson approximation that is well justified for ^{150}Nd , ^{160}Gd , and ^{160}Dy , which indeed reveal strong deformations. As for ^{150}Sm , the enhanced quadrupole moment of this nucleus is an indication for its static deformation. Nevertheless, the experimental level schemes

of ^{150}Sm , as well as of ^{76}Ge and ^{76}Se , do not reveal clear ground-state rotational bands. A more elaborated theoretical treatment going beyond the simple adiabatic approximation might be needed in the future to describe the nuclear dynamics of ^{150}Sm , ^{76}Ge , and ^{76}Se . For instance, the so-called weak coupling, or no alignment, limit [20] seems to be more suitable for ^{76}Ge and ^{76}Se as having rather small deformations. In this limit, the Coriolis force becomes so strong that the angular momenta of the valence nucleons get completely decoupled from the orientation of the core. Another important question is the relevance that an exact angular momentum projection could have. All these cases deserve a separate detailed study, and the adiabatic approach to the description of excited states of all the nuclei in question is adopted in the present application of the QRPA with a realistic residual interaction.

Though it is difficult to evaluate the effects beyond the adiabatic approximation employed here, one might anticipate already without calculations that the smaller the deformation is, the smaller should be the deviation of the calculated observables from the ones obtained in the spherical limit. In this connection it is worth noting that spherical QRPA results can exactly be reproduced in the present calculation by letting deformation vanish, in spite of the formal inapplicability of the adiabatic ansatz for the wave function in this limit.

Nuclear excitations in the intrinsic system $|K^\pi\rangle$ are characterized by the projection of the total angular momentum onto the nuclear symmetry axis K (the only projection which is conserved in strongly deformed nuclei) and the parity π . In Ref. [16] the structure of the intermediate $|0^+\rangle$ and $|1^+\rangle$ states was obtained within the QRPA to calculate $2\nu\beta\beta$ -decay NME $M^{2\nu}$. Here, the approach of Ref. [16] is straightforwardly extended to calculate all possible $|K^\pi\rangle$ states needed to construct the NME $M^{0\nu}$.

The intrinsic states $|K^\pi, m\rangle$ are generated within the QRPA by a phonon creation operator acting on the ground-state wave function:

$$|K^\pi, m\rangle = Q_{m,K}^\dagger |0_{\text{g.s.}}^+\rangle; \quad (4)$$

$$Q_{m,K}^\dagger = \sum_{pn} X_{pn,K}^m A_{pn,K}^\dagger - Y_{pn,K}^m \bar{A}_{pn,K}.$$

Here, $A_{pn,K}^\dagger = a_p^\dagger a_n^\dagger$ and $\bar{A}_{pn,K} = a_{\bar{p}} a_n$ are the two-quasiparticle creation and annihilation operators, respectively, with the bar denoting the time-reversal operation. The quasiparticle pairs $p\bar{n}$ are defined by the selection rules $\Omega_p - \Omega_n = K$ and $\pi_p \pi_n = \pi$, where π_τ is the single-particle (s.p.) parity and Ω_τ is the projection of the total s.p. angular momentum on the nuclear symmetry axis ($\tau = p, n$). The s.p. states $|p\rangle$ and $|n\rangle$ of protons and neutrons are calculated by solving the Schrödinger equation with the deformed axially symmetric Woods-Saxon potential [16]. In the cylindrical coordinates, the deformed Woods-Saxon s.p. wave functions $|\tau \Omega_\tau\rangle$ with $\Omega_\tau > 0$ are decomposed over the deformed harmonic oscillator s.p. wave functions (with the principal quantum numbers $N n_z \Lambda$) and the spin wave functions $|\Sigma = \pm \frac{1}{2}\rangle$:

$$|\tau \Omega_\tau\rangle = \sum_{N n_z \Sigma} b_{N n_z \Sigma} |N n_z \Lambda_\tau = \Omega_\tau - \Sigma\rangle |\Sigma\rangle, \quad (5)$$

where $N = n_\perp + n_z$ ($n_\perp = 2n_\rho + |\Lambda|$), n_z and n_ρ are the number of nodes of the basis functions in the z and ρ directions, respectively; $\Lambda = \Omega - \Sigma$ and Σ are the projections of the orbital and spin angular momentum onto the symmetry axis z . For the s.p. states with the negative projection $\Omega_\tau = -|\Omega_\tau|$, which are degenerate in energy with $\Omega_\tau = |\Omega_\tau|$, the time-reversed version of Eq. (5) is used as a definition (see also Ref. [16]). The states $(\tau, \bar{\tau})$ comprise the whole single-particle model space.

The deformed harmonic oscillator wave functions $|Nn_z\Lambda\rangle$ can be further decomposed over the spherical harmonic oscillator ones $|n_r l \Lambda\rangle$ by calculating the corresponding spatial overlap integrals $A_{Nn_z\Lambda}^{n_r l} = \langle n_r l \Lambda | Nn_z \Lambda \rangle$ (n_r is the radial quantum number, l and Λ are the orbital angular momentum and its projection onto z axes, respectively), see Appendix of Ref. [16] for more details. Thereby, the wave function (5) can be reexpressed as

$$|\tau \Omega_\tau\rangle = \sum_{\eta} B_{\eta}^{\tau} |\eta \Omega_\tau\rangle, \quad (6)$$

where $|\eta \Omega_\tau\rangle = \sum_{\Sigma} C_{|\Omega_\tau - \Sigma| \frac{1}{2} \Sigma}^{j \Omega_\tau} |n_r l \Lambda = \Omega_\tau - \Sigma\rangle |\Sigma\rangle$ is the spherical harmonic oscillator wave function in the j -coupled scheme [$\eta = (n_r l j)$], and $B_{\eta}^{\tau} = \sum_{\Sigma} C_{|\Omega_\tau - \Sigma| \frac{1}{2} \Sigma}^{j \Omega_\tau} A_{Nn_z\Omega_\tau - \Sigma}^{n_r l} b_{Nn_z \Sigma}$, with $C_{|\Omega_\tau - \Sigma| \frac{1}{2} \Sigma}^{j \Omega_\tau}$ being the Clebsch-Gordan coefficient.

The QRPA equations:

$$\begin{pmatrix} \mathcal{A}(K) & \mathcal{B}(K) \\ -\mathcal{B}(K) & -\mathcal{A}(K) \end{pmatrix} \begin{pmatrix} X_K^m \\ Y_K^m \end{pmatrix} = \omega_{K,m} \begin{pmatrix} X_K^m \\ Y_K^m \end{pmatrix}, \quad (7)$$

with realistic residual interaction are solved to get the forward X_{iK}^m , backward Y_{iK}^m amplitudes and the excitation energies ω_K^m and ω_K^m of the m th K^π state in the intermediate nucleus. The matrix \mathcal{A} and \mathcal{B} are defined by

$$\begin{aligned} \mathcal{A}_{pn,p'n'}(K) &= \delta_{pn,p'n'}(E_p + E_n) + g_{pp}(u_p u_n u_{p'} u_{n'} + v_p v_n v_{p'} v_{n'}) V_{p\bar{n}p'\bar{n}'} \\ &\quad - g_{ph}(u_p v_n u_{p'} v_{n'} + v_p u_n v_{p'} u_{n'}) V_{pn'p'n} \\ \mathcal{B}_{pn,p'n'}(K) &= -g_{pp}(u_p u_n v_{p'} v_{n'} + v_p v_n u_{p'} u_{n'}) V_{p\bar{n}p'\bar{n}'} \\ &\quad - g_{ph}(u_p v_n v_{p'} v_{n'} + v_p u_n u_{p'} u_{n'}) V_{pn'p'n}, \end{aligned} \quad (8)$$

where $E_p + E_n$ are the two-quasiparticle excitation energies, $V_{pn,p'n'}$ and $V_{p\bar{n},p'\bar{n}'}$ are the particle-hole (ph) and particle-particle (pp) matrix elements of the residual nucleon-nucleon interaction V , respectively, u_τ and v_τ are the coefficients of the Bogoliubov transformation.

As a residual two-body interaction, we use the nuclear Brueckner G matrix, which is a solution of the Bethe-Goldstone equation, derived from the charge-dependent Bonn (Bonn-CD) one boson exchange potential, as used also in the spherical calculations of Ref. [7]. The G matrix elements are originally calculated with respect to a spherical harmonic oscillator s.p. basis. By using the decomposition of the deformed s.p. wave function in Eq. (6), the two-body deformed wave function can be represented as

$$|p\bar{n}\rangle = \sum_{\eta_p \eta_n J} F_{p\eta_p n \eta_n}^{JK} |\eta_p \eta_n, JK\rangle, \quad (9)$$

where $|\eta_p \eta_n, JK\rangle = \sum_{m_p m_n} C_{j_p m_p j_n m_n}^{JK} |\eta_p m_p\rangle |\eta_n m_n\rangle$, and $F_{p\eta_p n \eta_n}^{JK} = B_{\eta_p}^p B_{\eta_n}^n (-1)^{j_n - \Omega_n} C_{j_p \Omega_p j_n - \Omega_n}^{JK}$ is defined for the sake of simplicity [$(-1)^{j_n - \Omega_n}$ is the phase arising from the time-reversed states $|\bar{n}\rangle$]. The particle-particle $V_{p\bar{n},p'\bar{n}'}$ and particle-hole $V_{pn',p'n}$ interaction matrix elements in the representation (8) for the QRPA matrices \mathcal{A}, \mathcal{B} [Eq. (7)] in the deformed Woods-Saxon single-particle basis can then be given in terms of the spherical G matrix elements as follows:

$$V_{p\bar{n},p'\bar{n}'} = -2 \sum_J \sum_{\eta_p \eta_n} \sum_{\eta_{p'} \eta_{n'}} F_{p\eta_p n \eta_n}^{JK} F_{p'\eta_{p'} n' \eta_{n'}}^{JK} G(\eta_p \eta_n \eta_{p'} \eta_{n'}, J), \quad (10)$$

$$V_{pn',p'n} = 2 \sum_J \sum_{\eta_p \eta_n} \sum_{\eta_{p'} \eta_{n'}} F_{p\eta_p n' \eta_{n'}}^{JK'} F_{p'\eta_{p'} n \eta_n}^{JK'} G(\eta_p \eta_{n'} \eta_{p'} \eta_n, J), \quad (11)$$

where $K'_{pn'} = \Omega_p + \Omega_{n'} = \Omega_{p'} + \Omega_n$.

The matrix element M^{0v} is given within the QRPA in the intrinsic system by a sum of the partial amplitudes of transitions via all the intermediate states K^π :

$$M^{0v} = \sum_{K^\pi} M^{0v}(K^\pi), \quad M^{0v}(K^\pi) = \sum_{\alpha} s_{\alpha}^{(\text{def})} O_{\alpha}(K^\pi). \quad (12)$$

Here, we use the notation of Appendix B in Ref. [21], α stands for the set of four single-particle indices $\{p, p', n, n'\}$, and $O_{\alpha}(K^\pi)$ is a two-nucleon transition amplitude via the K^π states in the intrinsic frame:

$$\begin{aligned} O_{\alpha}(K^\pi) &= \sum_{m_i, m_f} \langle 0_f^+ | c_p^\dagger c_n | K^\pi m_f \rangle \langle K^\pi m_f | K^\pi m_i \rangle \\ &\quad \times \langle K^\pi m_i | c_{p'}^\dagger c_{n'} | 0_i^+ \rangle. \end{aligned} \quad (13)$$

The two sets of intermediate nuclear states generated from the initial and final g.s. (labeled by m_i and m_f , respectively) do not come out identical within the QRPA. A standard way to tackle this problem is to introduce in Eq. (13) the overlap factor of these states $\langle K^\pi m_f | K^\pi m_i \rangle$, whose representation is given below, Eq. (16). Two-body matrix elements $s_{\alpha}^{(\text{def})}$ of the neutrino potential in Eq. (12) in a deformed Woods-Saxon single-particle basis are decomposed over the spherical harmonic oscillator ones according to Eqs. (9) and (11):

$$\begin{aligned} s_{pp'n'n'}^{(\text{def})} &= \sum_J \sum_{\eta_p \eta_{p'} \eta_n \eta_{n'}} F_{p\eta_p n \eta_n}^{JK} F_{p'\eta_{p'} n' \eta_{n'}}^{JK} s_{\eta_p \eta_{p'} \eta_n \eta_{n'}}^{(\text{sph})}(J), \quad (14) \\ s_{pp'n'n'}^{(\text{sph})}(J) &= \sum_{\mathcal{J}} (-1)^{j_n + j_{p'} + J + \mathcal{J}} \hat{\mathcal{J}} \begin{Bmatrix} j_p & j_n & J \\ j_{n'} & j_{p'} & \mathcal{J} \end{Bmatrix} \\ &\quad \times \langle p(1), p'(2); \mathcal{J} | \mathcal{O}_{\ell}(1, 2) | n(1), n'(2); \mathcal{J} \rangle, \end{aligned} \quad (15)$$

where $\hat{\mathcal{J}} \equiv \sqrt{2\mathcal{J} + 1}$, and $\mathcal{O}_{\ell}(1, 2)$ is the neutrino potential as a function of coordinates of two particles, with ℓ labeling its Fermi (F), Gamow-Teller (GT), and tensor (T) parts.

The particle-hole transition amplitudes in Eq. (13) can be represented in terms of the QRPA forward X_{iK}^m and backward Y_{iK}^m amplitudes along with the coefficients of the Bogoliubov

transformation u_τ and v_τ [16]:

$$\begin{aligned}\langle 0_f^+ | c_p^\dagger c_n | K^\pi m_f \rangle &= v_p u_n X_{pn, K^\pi}^{m_f} + u_p v_n Y_{pn, K^\pi}^{m_f}, \\ \langle K^\pi m_i | c_p^\dagger c_n | 0_i^+ \rangle &= u_p v_n X_{pn, K^\pi}^{m_i} + v_p u_n Y_{pn, K^\pi}^{m_i}.\end{aligned}$$

The overlap factor in Eq. (13) can be written as

$$\begin{aligned}\langle K^\pi m_f | K^\pi m_i \rangle &= \sum_{l_i l_f} [X_{l_f K^\pi}^{m_f} X_{l_i K^\pi}^{m_i} - Y_{l_f K^\pi}^{m_f} Y_{l_i K^\pi}^{m_i}] \\ &\times \mathcal{R}_{l_f l_i}(\text{BCS}_f | \text{BCS}_i).\end{aligned}\quad (16)$$

Representations for $\mathcal{R}_{l_f l_i}$ and the overlap factor $\langle \text{BCS}_f | \text{BCS}_i \rangle$ between the initial and final BCS vacua are given in Ref. [14].

III. RESULTS AND ANALYSIS

We have computed the NME $M^{0\nu}$ for the $0\nu\beta\beta$ decays $^{76}\text{Ge} \rightarrow ^{76}\text{Se}$, $^{150}\text{Nd} \rightarrow ^{150}\text{Sm}$, and $^{160}\text{Gd} \rightarrow ^{160}\text{Dy}$. The single-particle Schrödinger equation with the Hamiltonian of a deformed Woods-Saxon mean field is solved on the basis of an axially deformed harmonic oscillator. The parametrization of the mean field is adopted from the spherical calculations of Refs. [7,21,22]. We use here the single-particle deformed basis corresponding in the spherical limit to full $(4-6)\hbar\omega$ shells. Decomposition of the deformed single-particle wave functions is performed over the spherical harmonic oscillator states within the seven major shells. Only quadrupole deformation is taken into account in the calculation. The geometrical quadrupole deformation parameter β_2 of the deformed Woods-Saxon mean field is obtained by fitting the experimental deformation parameter $\beta = \sqrt{\frac{\pi}{5}} \frac{Q_p}{Z r_c^2}$, where r_c is the charge rms radius and Q_p is the empirical intrinsic quadrupole moment. The latter can be derived from the laboratory quadrupole moments measured by the Coulomb excitation reorientation technique, or from the corresponding $B(E2)$ values [23]. We take in this work experimental values extracted from the $B(E2)$ values as being more accurate. The fitted values of the parameter β_2 of the deformed Woods-Saxon mean field, which allow us to reproduce the experimental β , are listed in Table I.

TABLE I. Values of the deformation parameter of Woods-Saxon mean field β_2 for initial (final) nuclei fitted in the calculation to reproduce the experimental quadrupole moment (labeled as “1”). The spherical limit is labeled as “0”. Also the fitted values of the particle-particle strength parameter g_{pp} are listed [for both cases without (I) and with (II) quenching of g_A]. The particle-hole strength parameter is $g_{ph} = 0.90$. The BCS overlap factor $\langle \text{BCS}_f | \text{BCS}_i \rangle$ (16) between the initial and final BCS vacua is given in the last column.

Initial (final) nucleus	β_2	g_{pp} (I)	g_{pp} (II)	$\langle \text{BCS}_i \text{BCS}_f \rangle$
^{76}Ge (^{76}Se)	0.10 (0.16) “1”	0.71	0.66	0.74
	0.0 (0.0) “0”	0.68	0.63	0.81
^{150}Nd (^{150}Sm)	0.240 (0.153) “1”	1.05	1.00	0.52
	0.0 (0.0) “0”	1.01	0.99	0.85
^{160}Gd (^{160}Dy)	0.303 (0.292) “1”	1.00 ^a	1.00	0.74

^aAs there is no experimental value of $M^{2\nu}$ for ^{160}Gd , we do not renormalize the p-p interaction and use $g_{pp} = 1$.

We label these sets of parameters as “1”. The spherical limit, i.e., $\beta_2 = 0$, is considered as well (labeled as “0”), to compare with the earlier results of Ref. [7]. The procedure adopted here of fitting β_2 is more consistent than the approximate ansatz $\beta_2 = \beta$ used in Ref. [16].

As in Refs. [7,16,18,21,22], the nuclear Brueckner G matrix, obtained by a solution of the Bethe-Goldstone equation with the Bonn-CD one boson exchange nucleon-nucleon potential, is used as a residual two-body interaction. First, the BCS equations are solved to obtain the Bogoliubov coefficients, gap parameter, and chemical potentials. The number N_{K^π} of the proton-neutron quasiparticle pairs coupled to a given K^π determines the dimension of the corresponding QRPA equations. It becomes the largest for $K^\pi = 0^+$ and is $N_{0^+} = 840$ for Ge and Se, and $N_{0^+} = 912$ for Nd, Sm, Gd, and Dy. To solve the QRPA equations, one has to fix the particle-hole g_{ph} and particle-particle g_{pp} renormalization factors of the residual interaction, Eqs. (8). As in Refs. [16,18], we determine a value of g_{ph} by fitting the experimental position of the Gamow-Teller giant resonance (GTR) in the intermediate nucleus. Since there is no experimental information on the GTR energy for ^{150}Nd , we use for this nucleus the same $g_{ph} = 0.90$ as fitted for ^{76}Ge (this value is slightly different from the fitted $g_{ph} = 1.15$ of Ref. [16] because of a different parametrization of the mean field used here). The parameter g_{pp} can be determined by fitting the experimental value of the $2\nu\beta\beta$ -decay NME $M_{GT}^{2\nu} = 0.07 \text{ MeV}^{-1}$ [17]. To account for the quenching of the axial-vector coupling constant g_A , we choose in the calculation, along with the bare value $g_A = 1.25$, also the quenched value $g_A^{\text{qch}} = 0.75g_A = 0.94$, where the quenching factor of 0.75 comes from a recent experimental measurement of GT strength distribution in ^{150}Nd [24]. The two sets of the fitted values of g_{pp} corresponding to the cases without or with quenching of g_A are listed Table I as cases (I) and (II), respectively. Note, that the more realistic procedure of fitting β_2 adopted here also gives us more realistic $g_{pp} \simeq 1$ values than those of Ref. [16].

Having solved the QRPA equations, the two-nucleon transition amplitudes (13) are calculated, and by combining them with the two-body matrix elements of the neutrino potential, the total $0\nu\beta\beta$ NME $M^{0\nu}$ (12) is formed. The present computation is rather time consuming since numerous programming loops are needed to calculate the decompositions of the two-body matrix elements in the deformed basis over the spherical ones. Therefore, to speed up the calculations the mean energy of 7 MeV of the intermediate states is used in the neutrino propagator. Following Refs. [7,21,22], we have taken into account the effects of the finite nucleon size, and higher-order weak currents are included. Recently, it was shown [22] that a modern self-consistent treatment of the two-nucleon short-range correlations (s.r.c.) leads to a change in the NME $M^{0\nu}$ only by a few percent, much less than the traditional Jastrow-type representation of the s.r.c. does. A very similar effect is found in the present calculation (see below).

We start our discussion of the calculated $0\nu\beta\beta$ -decay NME by a comparison of the matrix elements of this work obtained in the spherical limit with the previous ones of Refs. [7,21,22], which provides an important cross-check of the present calculation. Though formally the adiabatic

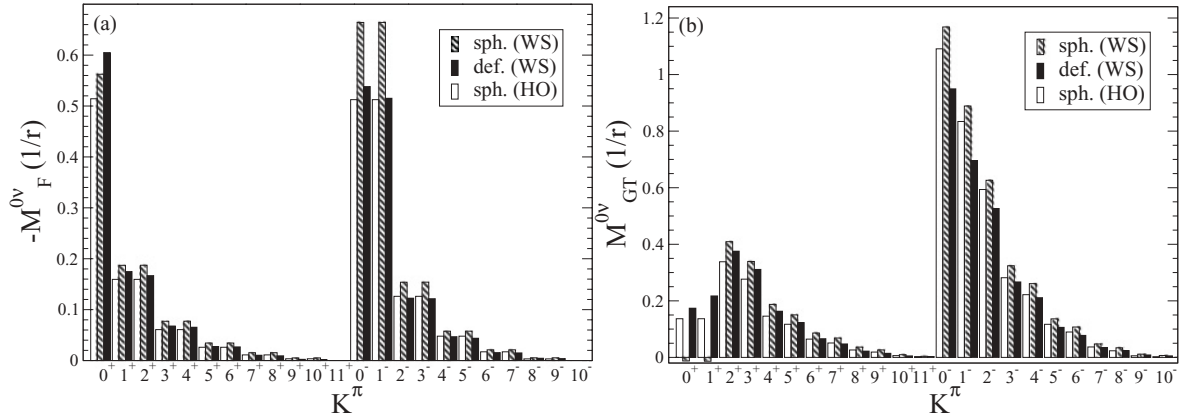


FIG. 1. The partial contributions $M^{0v}(K^\pi)$ of different intermediate K^π states to $M^{0v}(1/r)$ for $^{150}\text{Nd} \rightarrow ^{150}\text{Sm}$ in the cases of vanishing and realistic deformations. For simplicity, the BCS overlap factor is omitted in these results. The Fermi $M_F^{0v}(1/r)$ and the GT $M_{GT}^{0v}(1/r)$ contributions are shown in the panels (a) and (b), respectively. The three bars represent (from left to right) the results obtained with the spherical harmonic oscillator (HO) wave functions, with the Woods-Saxon (WS) wave functions in the spherical limit, and with the deformed WS wave functions for realistic deformations from Table I.

Bohr-Mottelson approximation is not applicable in the limit of vanishing deformation, it is easy to see that the basic Eqs. (12)–(16) do have the correct spherical limit.

According to Eq. (12), the total calculated $0\nu\beta\beta$ -decay NME is formed by the sum of all partial contributions $M^{0v}(K^\pi)$ of different intrinsic intermediate states K^π , with $M^{0v}(|K|^\pi) = M^{0v}(-|K|^\pi)$. In the spherical limit, the total angular momentum J becomes a good quantum number, and the intermediate K^π states corresponding to a given J^π state become degenerate. In addition, in this limit, each projection K of an intermediate J^π state contributes equally to the calculated $0\nu\beta\beta$ -decay NME, as a consequence of rotational symmetry. To represent standard spherical results in the terms of the present paper, one has to use the following expression for the spherical partial contribution of a projection K : $M^{0v}(K^\pi) = \sum_{J \geq |K|} M^{0v}(J^\pi)/(2J+1)$; it is easy to see that having summed over all K^π , one obtains the total NME

$M^{0v} = \sum_J M^{0v}(J^\pi)$. From this representation it can generally be expected that the smaller is $|K|$, the larger the corresponding partial contribution $M^{0v}(K^\pi)$ should be (since simply more J 's contribute, and their contributions are of the same sign in most cases, see Ref. [7]). This behavior is in fact revealed by most of the calculation results (see below).

To test our new numerical code calculating $0\nu\beta\beta$ -decay NME for deformed nuclei, we have taken the spherical limit and used in it the spherical harmonic oscillator wave functions as usually done in the QRPA calculations [7,21,22]. The NME calculated by different codes are found to be in an excellent agreement.

For the further discussion, we define the following contributions to the total $0\nu\beta\beta$ -decay NME: $M_F^{0v}(1/r)$ and $M_{GT}^{0v}(1/r)$ are calculated by taking into account only the Coulomb-like radial dependence of the neutrino potential. The total corrections ΔM_F^{0v} and ΔM_{GT}^{0v} to $M_F^{0v}(1/r)$ and $M_{GT}^{0v}(1/r)$,

TABLE II. Different contributions to the total calculated NME M^{0v} for $0\nu\beta\beta$ decays $^{76}\text{Ge} \rightarrow ^{76}\text{Se}$, $^{150}\text{Nd} \rightarrow ^{150}\text{Sm}$, and $^{160}\text{Gd} \rightarrow ^{160}\text{Dy}$. The BCS overlap is taken into account. In columns 4 and 9 the leading contributions $M_F(1/r)$ and $M_{GT}(1/r)$ are shown. In columns 5 and 10 the total corrections ΔM_F and ΔM_{GT} to $M_F(1/r)$ and $M_{GT}(1/r)$ are listed. In columns 6,7 and 11,12 the corrections $\delta_1 M_F$ and $\delta_1 M_{GT}$, respectively, coming from different choices of the s.r.c., are listed. In columns 8 and 13 both the F and GT parts of the total NME (17) are shown (we prefer here the final value of M^{0v} corresponding to the modern self-consistent treatment of the s.r.c. [22]). Finally, in columns 14 and 15 the $0\nu\beta\beta$ -decay NME M^{0v} (3) and corresponding decay half-lives (assuming $m_{\beta\beta} = 50$ meV) are listed.

A	Def.	g_A	M_F^{0v}					M_{GT}^{0v}					M^{0v}	$T_{1/2}^{0v} (10^{26} \text{ yr})$ ($m_{\beta\beta} = 50 \text{ meV}$)
			$M(1/r)$	ΔM	$\delta_1 M$	$\delta_2 M$	Total	$M(1/r)$	ΔM	$\delta_1 M$	$\delta_2 M$	Total		
76	“1”	1.25	-2.83	0.69	0.40	-0.08	-2.22	5.59	-2.49	-0.88	0.18	3.27	4.69	7.15
		0.94	-2.98	0.73	0.40	-0.18	-2.44	7.69	-3.65	-1.47	0.27	4.31	4.00	9.83
	“0”	1.25	-3.15	0.78	0.45	-0.09	-2.47	6.37	-2.85	-1.01	0.20	3.72	5.30	5.60
		0.94	-3.31	0.82	0.46	-0.10	-2.59	7.28	-3.15	-1.04	0.21	4.35	4.10	9.36
150	“1”	1.25	-2.09	0.51	0.33	-0.06	-1.64	4.01	-1.86	-0.72	0.14	2.29	3.34	0.41
		0.94	-2.16	0.52	0.33	-0.06	-1.70	4.44	-2.00	-0.73	0.14	2.58	2.55	0.71
	“0”	1.25	-4.07	0.99	0.67	-0.13	-3.21	7.35	-3.54	-1.46	0.26	4.07	6.12	0.12
		0.94	-4.12	1.00	0.68	-0.13	-3.25	7.69	-3.65	-1.47	0.27	4.31	4.52	0.23
160	“1”	1.25	-2.14	0.51	0.32	-0.07	-1.69	4.57	-2.04	-0.71	0.14	2.67	3.76	2.26

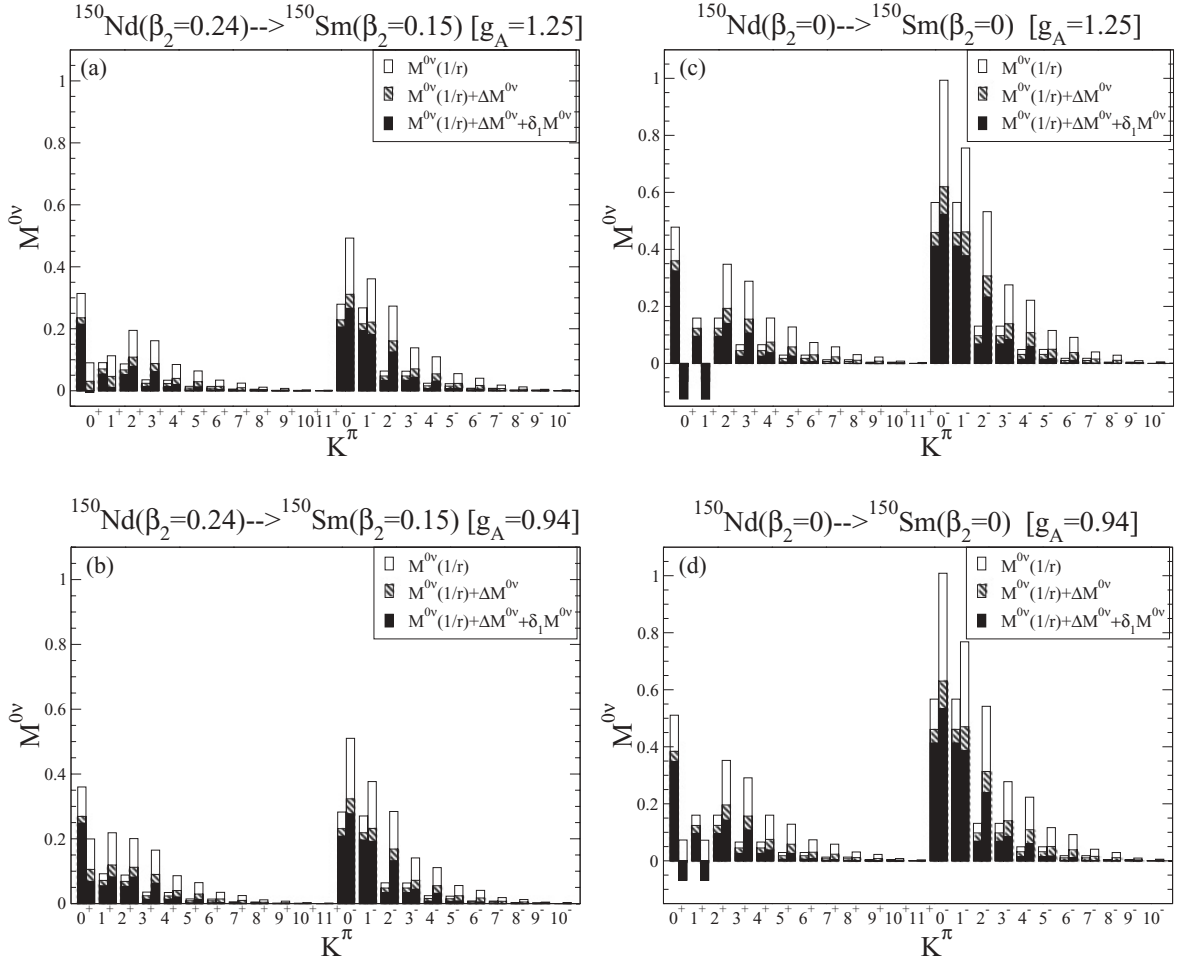


FIG. 2. Partial contributions $M^{0\nu}(K^\pi)$ of different intrinsic intermediate states to the total $M^{0\nu}$ for $^{150}\text{Nd} \rightarrow ^{150}\text{Sm}$ in the case of realistic deformation [panels (a) and (b)] and in the spherical limit [(c) and (d)]. The Fermi $-M_F^{0\nu}(K^\pi)$ and $GT M_{GT}^{0\nu}(K^\pi)$ contributions are shown for each K^π by the left and right bars, respectively. The contributions include the leading, Coulomb-like, radial dependence of the neutrino potential [labeled “ $M(1/r)$ ”], with the effects of the FNS, the closure energy, and higher-order weak currents included [labeled “ $M(1/r) + \Delta M$ ”], and the final contributions, including in addition the effect of the Jastow-like s.r.c. [labeled “ $M(1/r) + \Delta M + \delta_1 M$ ”]. The panels (a),(c) and (b),(d) show the results corresponding to the unquenched $g_A = 1.25$ and quenched $g_A = 0.94$, respectively [fitted values (I) and (II) of g_{pp} , see Table I].

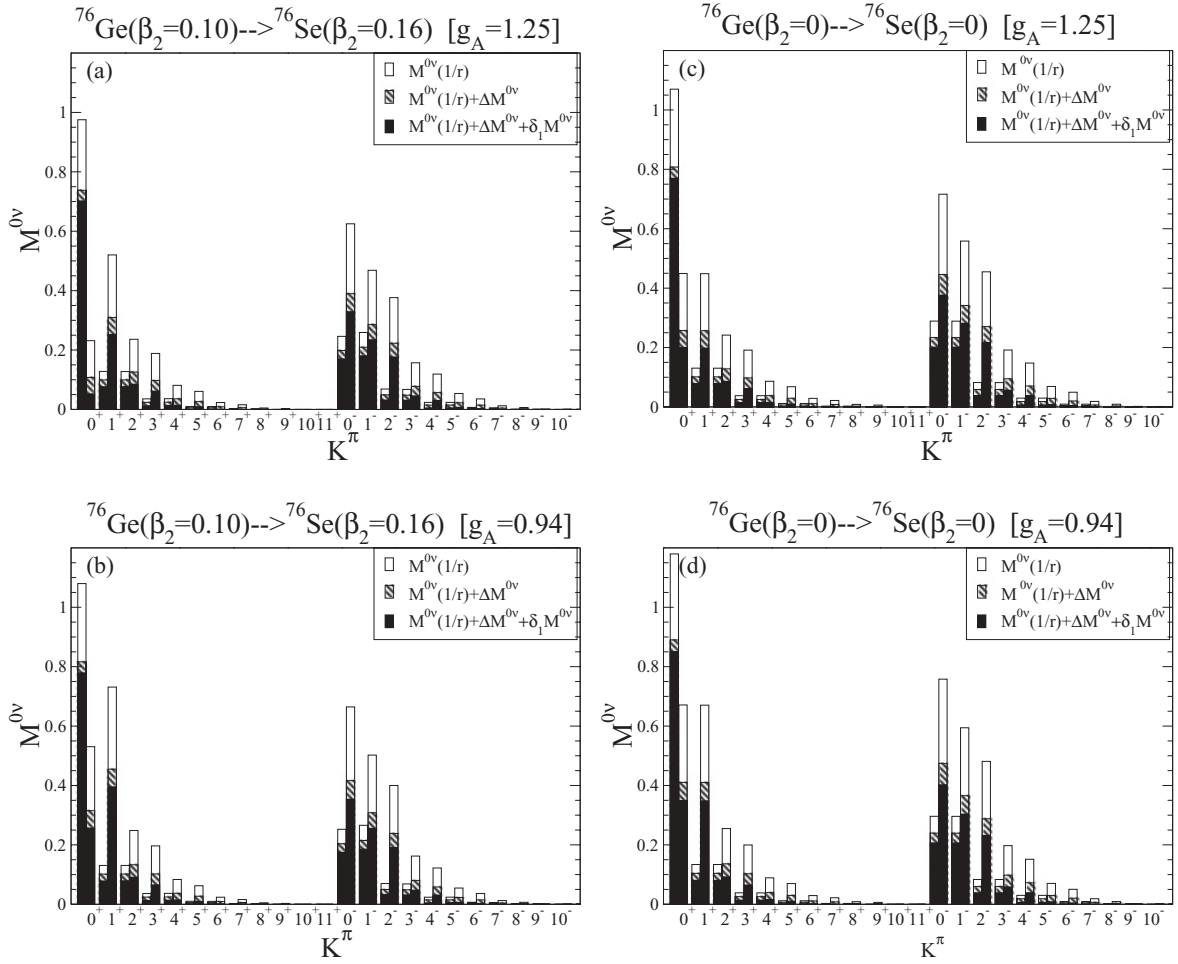
respectively, come from the effects of the finite nucleon size (FNS), the closure energy, and higher-order weak currents. Finally, the corrections $\delta_i M_F^{0\nu}$ and $\delta_i M_{GT}^{0\nu}$, respectively, come from the effects of the s.r.c. (Jastow-like s.r.c. is denoted by the subscript $i = 1$, and the self-consistent Bonn-CD s.r.c. by the subscript $i = 2$). Thus, the final total $0\nu\beta\beta$ -decay NME is given by

$$M^{0\nu} = M^{0\nu}(1/r) + \Delta M^{0\nu} + \delta_i M^{0\nu}. \quad (17)$$

The effect of deformation and different choices of the single-particle wave functions on the partial contributions $M^{0\nu}(K^\pi)$ of different K^π intermediate states to $M^{0\nu}(1/r)$ for ^{150}Nd is illustrated in Fig. 1. The BCS overlap factor is neglected here for simplicity. The Fermi and the GT contributions are shown in the left and right panels of the figure, respectively. The left and middle bars for each K^π represent the results obtained for zero deformation with the spherical harmonic oscillator wave functions and with the Woods-Saxon wave functions,

respectively, and the right bar represents the result calculated with the deformed Woods-Saxon wave functions for the finite deformations from Table I (case “1”). Each bar for $K > 0$ represents a sum of the equal contributions of the positive and negative projections, $M^{0\nu}(K^\pi) + M^{0\nu}(-K^\pi) = 2M^{0\nu}(K^\pi)$. Because the partial contributions $M_F^{0\nu}(K^\pi)$ to the Fermi NME in the spherical limit are nonzero only for the intermediate states of natural parity $\pi = (-1)^J$, the equality $M_F^{0\nu}(K^\pi, \pi = (-1)^K) = M_F^{0\nu}((K-1)^\pi, \pi = (-1)^K)$ ($K > 0$) should hold in this limit (this simply reflects equality of the contributions of different projections K for a given J). This equality is nicely fulfilled in our calculations, as illustrated by Fig. 1. Also, one can see in Fig. 1 that even for rather large deformations, the partial contributions $M^{0\nu}(K^\pi)$ (calculated with neglect of the BCS overlap) do not differ much from the corresponding ones of the spherical calculations. The corresponding results for the other nuclei show very similar pattern.

The final results for the NME for $0\nu\beta\beta$ decays $^{76}\text{Ge} \rightarrow ^{76}\text{Se}$, $^{150}\text{Nd} \rightarrow ^{150}\text{Sm}$, and $^{160}\text{Gd} \rightarrow ^{160}\text{Dy}$ are listed in Table II (now

FIG. 3. Same as in Fig. 2, but for $^{76}\text{Ge} \rightarrow ^{76}\text{Se}$.

the values of the BCS overlap from the last column of Table I are taken into account). In columns 4 and 9, the leading contributions $M_F(1/r)$ and $M_{GT}(1/r)$ are shown. In columns 5 and 10, the total corrections ΔM_F and ΔM_{GT} to $M_F(1/r)$ and $M_{GT}(1/r)$ are listed. One sees that these corrections reduce the results of the leading order by about 20% for the Fermi part and 40% for the GT part, which agrees with the previous spherical QRPA calculations [25]. In columns 6 and 7 and 11 and 12, the corrections $\delta_{1,2}M_F$ and $\delta_{1,2}M_{GT}$, respectively, coming from different choices of the s.r.c., are listed. In columns 8 and 13, both the F and GT parts of the total NME $M_\ell^{0v} = M_\ell^{0v}(1/r) + \Delta M_\ell^{0v} + \delta_2 M_\ell^{0v}$ are shown (we prefer here the final value of M^{0v} corresponding to the modern self-consistent treatment of the s.r.c. [22]). Finally, in columns 14 and 15, the $0\nu\beta\beta$ -decay NME M^{0v} (3) and corresponding decay half-lives (assuming $m_{\beta\beta} = 50$ meV) are listed. The corresponding K^π decompositions of M^{0v} are shown in Figs. 2 and 3.

By inspecting Table II and Figs. 2 and 3, one sees that the difference between the spherical and deformed results mainly come from the BSC overlap between the ground states of the initial and final nuclei. As for the g_{pp} dependence of the $0\nu\beta\beta$ -decay NME, it is much less pronounced than the dependence of the amplitude of $2\nu\beta\beta$ decay. A marked reduction of the

total M^{0v} for the quenched value of g_A can be traced back to a smaller prefactor $(g_A/1.25)^2$ in the definition of M^{0v} (3).

The strongest effect of deformation on M^{0v} (the suppression by about 40% as compared to our previous QRPA result obtained with neglect of deformation) is found in the case of ^{150}Nd . This suppression can be traced back to a rather large difference in deformations of the ground states of ^{150}Nd and ^{150}Sm . Such an effect has been observed also by other authors [8,10,11]. The modern self-consistent treatment of the s.r.c. [22] makes the resulting $M^{0v} = 3.34$ (without quenching), even a bit larger than the NME $M^{0v} = 3.16$ of Ref. [18], where the influence of the s.r.c. was completely neglected. This translates to the half-life $T_{1/2}^{0v} = 4.1 \times 10^{25}$ yr for the effective Majorana neutrino mass $\langle m_{\beta\beta} \rangle = 50$ meV (cf. with $T_{1/2}^{0v} = 4.60 \times 10^{25}$ yr of Ref. [18]). In the case of quenched g_A , the half-life $T_{1/2}^{0v} = 7.1 \times 10^{25}$ yr is about twice longer as a consequence of a smaller NME $M^{0v} = 2.55$.

IV. CONCLUSIONS

In this paper a microscopic approach to calculation of the nuclear matrix element M^{0v} for neutrinoless double- β decay with an account for nuclear deformation is presented in length

and applied to calculate $M^{0\nu}$ for ^{76}Ge , ^{150}Nd and ^{160}Gd . The QRPA with a realistic residual interaction (the Brueckner G matrix derived from the Bonn-CD nucleon-nucleon potential) is used as the underlying nuclear structure model. The effects of the short-range correlations and the quenching of the axial vector coupling constant g_A are analyzed and found to be in accord with the spherical QRPA calculations. The strongest effect of deformation on $M^{0\nu}$ (the suppression by about 40% as compared to our previous QRPA result obtained with neglect of deformation) is found in the case of ^{150}Nd . This suppression can be traced back to a rather large difference in deformations of the ground states of ^{150}Nd and ^{150}Sm ,

which agrees with results by other authors. The preliminary conclusion of Ref. [18] that neutrinoless double- β decay of ^{150}Nd may provide one of the best probes of the Majorana neutrino mass is confirmed.

ACKNOWLEDGMENTS

The authors acknowledge the support of the Deutsche Forschungsgemeinschaft under both SFB TR27 “Neutrinos and Beyond” and Graduiertenkolleg GRK683. The work of F.Š. was also partially supported by the VEGA Grant agency under Contract No. 1/0249/03.

-
- [1] F. Boehm and P. Vogel, *Physics of Massive Neutrinos*, 2nd ed. (Cambridge University, Cambridge, England, 1992).
 - [2] A. Faessler and F. Šimkovic, *J. Phys. G* **24**, 2139 (1998); J. Suhonen and O. Civitarese, *Phys. Rep.* **300**, 123 (1998); S. R. Elliott and P. Vogel, *Annu. Rev. Nucl. Part. Sci.* **52**, 115 (2002); J. D. Vergados, *Phys. Rep.* **361**, 1 (2002); S. R. Elliott and J. Engel, *J. Phys. G* **30**, R183 (2004).
 - [3] Frank T. Avignone III, Steven R. Elliott, and Jonathan Engel, *Rev. Mod. Phys.* **80**, 481 (2008).
 - [4] J. Schechter and J. W. F. Valle, *Phys. Rev. D* **25**, 774 (1982).
 - [5] B. Kayser, *Phys. Lett. B* **667**, 1 (2008).
 - [6] C. Kraus and S. J. M. Peeters (SNO + Collaboration), *Prog. Part. Nucl. Phys.* **64**, 273 (2010); SNO+ project: [<http://snoplus.phy.queensu.ca>].
 - [7] V. A. Rodin, A. Faessler, F. Šimkovic, and P. Vogel, *Nucl. Phys. A* **766**, 107 (2006); **793**, 213(E) (2007).
 - [8] J. Menéndez, A. Poves, E. Caurier, and F. Nowacki, *Nucl. Phys. A* **818**, 139 (2009).
 - [9] J. G. Hirsch, O. Castanos, and O. Hess, *Nucl. Phys. A* **582**, 124 (1995).
 - [10] R. Chandra, J. Singh, P. K. Rath, P. K. Raina, and J. G. Hirsch, *Eur. Phys. J. A* **23**, 223 (2005); S. Singh, R. Chandra, P. K. Rath, P. K. Raina, and J. G. Hirsch, *ibid.* **33**, 375 (2007); K. Chaturvedi, R. Chandra, P. K. Rath, P. K. Raina, and J. G. Hirsch, *Phys. Rev. C* **78**, 054302 (2008).
 - [11] J. Barea and F. Iachello, *Phys. Rev. C* **79**, 044301 (2009).
 - [12] T. R. Rodriguez and G. Martinez-Pinedo, *Phys. Rev. Lett.* **105**, 252503 (2010).
 - [13] A. Escuderos, A. Faessler, V. Rodin, and F. Šimkovic, *J. Phys. G* **37**, 125108 (2010).
 - [14] F. Šimkovic, L. Pacearescu, and A. Faessler, *Nucl. Phys. A* **733**, 321 (2004).
 - [15] R. Alvarez-Rodriguez, P. Sarriguren, E. Moya de Guerra, L. Pacearescu, A. Faessler, and F. Šimkovic, *Phys. Rev. C* **70**, 064309 (2004).
 - [16] M. S. Yousef, V. Rodin, A. Faessler, and F. Šimkovic, *Phys. Rev. C* **79**, 014314 (2009); D. Fang, A. Faessler, V. Rodin, M. S. Yousef, and F. Šimkovic, *ibid.* **81**, 037303 (2010).
 - [17] A. S. Barabash, *Phys. Rev. C* **81**, 035501 (2010).
 - [18] D. L. Fang, A. Faessler, V. Rodin, and F. Šimkovic, *Phys. Rev. C* **82**, 051301(R) (2010).
 - [19] C. Amsler *et al.*, *Phys. Lett. B* **667**, 1 (2008).
 - [20] P. Ring and P. Schuck, *The Nuclear Many Body Problem* (Springer-Verlag, Berlin, 1980).
 - [21] F. Šimkovic, A. Faessler, V. A. Rodin, P. Vogel, and J. Engel, *Phys. Rev. C* **77**, 045503 (2008).
 - [22] F. Šimkovic, A. Faessler, H. Mütter, V. Rodin, and M. Stauf, *Phys. Rev. C* **79**, 055501 (2009).
 - [23] Chart of nucleus shape and size parameters [<http://cdfc.sinp.msu.ru/services/radchart/radmain.html>], and references therein.
 - [24] R. G. T. Zegers (private communication).
 - [25] F. Šimkovic, G. Pantis, J. D. Vergados, and A. Faessler, *Phys. Rev. C* **60**, 055502 (1999).